

Efficient Bayesian Inference for Spatial Point Patterns Using the Palm Likelihood

Kevin M. Collins*

Department of Statistics, North Carolina State University
and

Erin M. Schliep

Department of Statistics, North Carolina State University

July 24, 2025

Abstract

Bayesian inference for spatial point patterns is often hindered computationally by intractable likelihoods. In the frequentist literature, estimating equations utilizing pseudolikelihoods have long been used for simulation-free parameter estimation. One such pseudolikelihood based on the process of differences is known as the Palm likelihood. Utilizing notions of Bayesian composite likelihoods and generalized Bayesian inference, we develop a framework for the use of Palm likelihoods in a Bayesian context. Naive implementation of the Palm likelihood results in posterior undercoverage of model parameters. We propose two approaches to remedy this issue and calibrate the resulting posterior. Numerical simulations illustrate both the efficacy of the method in terms of statistical properties and the superiority in terms of computational efficiency when compared to classical Markov chain Monte Carlo. The method is then applied to the popular *Beilschmiedia pendula Lauraceae* dataset.

Keywords: point processes, log-Gaussian Cox process, generalized Bayes, pseudolikelihood

*This work is supported in part by U.S. Geological Survey Northeast and Southeast Climate Adaptation Science Center Grant No. G22AC00597-01.

1 Introduction

Spatial point pattern data arises in research areas such as ecology (Waagepetersen et al. 2016, Velázquez et al. 2016, Perry et al. 2006, Ben-Said 2021), biology (Weston et al. 2012, Burguet & Andrey 2014), criminology (Shirota & Gelfand 2017), seismology (D’Angelo et al. 2023), and public health (Diggle et al. 2013), and have been studied extensively by statisticians and probabilists. A general theoretical treatment of point processes can be found in Møller & Waagepetersen (2003), with emphasis on spatial point processes presented in Diggle (2013) and Baddeley et al. (2016). Statistical estimation and inferential methods for spatial point patterns are often complex and difficult to implement, which limits their utility. In particular, many of these methods are computationally intractable, requiring advanced algorithms for model fitting.

For point patterns, the likelihood itself is often intractable. Take, for example, the popular log-Gaussian Cox process (LGCP) (Møller et al. 1998). The likelihood requires integration over an infinite-dimensional random variable due to its doubly stochastic nature, requiring some form of approximation. Further, the assumption of a latent Gaussian process requires the inversion of a covariance matrix, which scales cubically in complexity with the dimension of the discretized process. One approach to subvert this intractability is through the optimization of an objective function simpler than the likelihood. Minimum contrast estimation (Baddeley et al. 2016) is a popular approach in the spirit of the method of moments applied to point processes. Letting $\boldsymbol{\theta}$ be the parameter of interest and u be the interpoint distance, an estimate $\hat{\boldsymbol{\theta}}$ is obtained by minimizing the discrepancy measure

$$D(\boldsymbol{\theta}) = \int_0^r \|\hat{J}(u)^c - J(u; \boldsymbol{\theta})^c\|^p du \quad (1)$$

for preselected constants r, c , and p where $J(\cdot)$ is a summary function, which has a closed form, such as the pair-correlation function or the K-function, and $\hat{J}(u)$ can be estimated nonparameterically. The primary advantage is that it is computationally simple to obtain

parameter estimates; however, the need to select the three tuning parameters is a drawback. Likelihood-based inference is often preferred by practitioners, but this can be costly. Computationally efficient likelihood-based methods have been developed based on the idea of composite likelihoods ([Lindsay 1988](#), [Varin et al. 2011](#)) or pseudolikelihoods ([Besag 1974](#)) in a number of different settings. One such example is semivariogram estimation in geostatistical models ([Curriero & Lele 1999](#), [Schliep et al. 2023](#)), which was extended to a spatiotemporal setting ([Bevilacqua et al. 2012](#)).

In the context of point patterns, [Baddeley & Turner \(2000\)](#) first developed a pseudolikelihood approach for Markov point processes. For cluster and Cox processes, [Guan \(2006\)](#) proposed a composite likelihood based on second-order intensities whereas the Palm likelihood based on palm intensities was developed by [Ogata & Katsura \(1991\)](#) and [Tanaka et al. \(2008\)](#). Each of these "likelihoods" is available in closed form, which dramatically improves computational performance. In the cases for point patterns, practitioners have only ever considered pairs of points when constructing the composite likelihood, leading to simplistic expressions. The drawback is that composite likelihoods result in a loss of information when compared to the full likelihood.

To date, these pseudolikelihood methods have been developed within the frequentist framework independent of the Bayesian literature. Classical Bayesian inference is an attractive approach to modeling point processes as the inherent hierarchical structure allows for the modeling of latent processes and enables full posterior inference with uncertainty propagation. Inference for Bayesian hierarchical models for point processes offer their own unique challenges, with computational difficulties often exacerbated by the iterative nature of Markov chain Monte Carlo (MCMC). Whereas the aforementioned frequentist approaches work for a general class of point processes, unique approaches for inference are required for specific classes of point processes. For example, when fitting an LGCP, one has to employ

an approach such as the Metropolis Adjusted Langevin Algorithm (Møller et al. 1998), Hamiltonian Monte Carlo (Betancourt 2017, Teng et al. 2017) or Elliptical slice sampling (Murray et al. 2010) in order to successfully explore the high-dimensional space of the latent Gaussian process. There has also been a push to develop deterministic computational strategies for LGCPs including INLA (Rue et al. 2017) and variational Bayes (Teng et al. 2017). As for inhibition and clustering processes, there is significantly less literature on Bayesian computation. Gelfand & Schliep (2018) advocate for the use of Approximate Bayesian Computation (ABC) for these classes of process. For Neyman-Scott processes, one has to take an approach such as the birth-death-move (Kopecký & Mrkvička 2016) in order to successfully sample from the parameter space.

Frequentists have adapted to the computational complexity of these models with likelihood approximations. Recently, a body of literature has been developing around replacing the likelihood in Bayesian computation with a simpler objective function. For example, Pauli et al. (2011) proposed the use of composite likelihoods in the Bayesian setting, and Ribatet et al. (2012) used the approach in a geostatistical context for extremes analysis. The notion of replacing the likelihood with another function that links the data to the parameters of interest (i.e. loss functions) has been studied in the literature as generalized Bayesian inference (Bissiri et al. 2016), Gibbs posteriors (Martin & Syring 2022), or Laplace-type estimators (Chernozhukov & Hong 2003). Importantly, Chernozhukov & Hong (2003) and Kleijn & Van der Vaart (2012) develop relevant Bernstein-von Mises results showing that the resulting posterior accumulates mass asymptotically around the estimator obtained from optimizing the objective function. Unfortunately, these results also show that resulting credible intervals provide inadequate coverage in terms of frequentist error rates. This requires calibration of the posterior/objective function (Wu & Martin 2023, Ribatet et al. 2012, Shaby 2014, Pauli et al. 2011) to control the error rate.

Our contribution in this paper is to extend the use of Palm likelihoods into a Bayesian framework for parameter inference in spatial point processes. We develop two different approaches to calibrating the resulting posteriors, which present unique challenges due to the nature of point patterns. Further, we develop an empirical Bayes approach based on the overall intensity of points that mimics the behavior of similar frequentist estimators. Throughout, we illustrate the efficacy of this generalized Bayesian approach in estimation, as well as the computational simplicity of our approach. The Palm likelihood enables direct sampling from the parameter spaces of these models with a simple random walk Metropolis-Hastings algorithm, saving the trouble of implementing different sampling schemes for unique classes of processes. Additionally, in contrast to INLA or variational Bayes, our approach is viable for multiple classes of point processes exhibiting different behaviors, not limited to those with a latent Gaussian process. This flexibility and simplicity of the Palm intensity expressions allows for easy model comparisons across a suite of different processes. In Section 2, we establish the necessary background on spatial point processes and the Palm likelihood. In Section 3, we discuss the implementation of Palm likelihoods in a Bayesian framework and develop algorithms for calibrating posterior uncertainty. Then, in Sections 4 and 5 we demonstrate the computational efficiency and inferential performance of our approach on simulated point patterns and a real data set, respectively. We conclude with a discussion of the work and future research in Section 6.

2 Palm Likelihood for Spatial Point Processes

2.1 Background

Let $\mathcal{S} = \{\mathbf{s}_1, \dots, \mathbf{s}_n\}$ be a spatial point pattern realized on the compact domain $\mathcal{D} \subset \mathbb{R}^2$ from a process indexed by parameter $\boldsymbol{\theta}$. For a region $B \subset \mathcal{D}$, let $N(B)$ denote the number

of points of \mathcal{S} in B . Let $d\mathbf{s}$ denote the infinitesimal ball around location \mathbf{s} and $|d\mathbf{s}|$ its area. The first-order intensity of the point pattern is defined as

$$\lambda(\mathbf{s}) = \lim_{|d\mathbf{s}| \rightarrow 0} \frac{E[N(d\mathbf{s})]}{|d\mathbf{s}|}, \quad (2)$$

where $\lambda(\mathbf{s})|d\mathbf{s}|$ is the probability of observing an event in $d\mathbf{s}$. Further, the probability that two points are observed at locations \mathbf{s}_i and \mathbf{s}_j is given by $\lambda_2(\mathbf{s}_i, \mathbf{s}_j)|d\mathbf{s}_i||d\mathbf{s}_j|$ where the second-order intensity is defined as

$$\lambda_2(\mathbf{s}_i, \mathbf{s}_j) = \lim_{|d\mathbf{s}_i|, |d\mathbf{s}_j| \rightarrow 0} \frac{E[N(d\mathbf{s}_i)N(d\mathbf{s}_j)]}{|d\mathbf{s}_i||d\mathbf{s}_j|}. \quad (3)$$

The conditional expression of the intensity of a point process, known as the Palm intensity (Coeurjolly et al. 2017), is written

$$\lambda_p(\mathbf{s}_i|\mathbf{s}_j) = \lambda_2(\mathbf{s}_i, \mathbf{s}_j)/\lambda(\mathbf{s}_j). \quad (4)$$

The Palm intensity times the area, $\lambda_p(\mathbf{s}_i|\mathbf{s}_j)|d\mathbf{s}_i|$, can be interpreted as the probability of observing an event at location \mathbf{s}_i given we observed an event at location \mathbf{s}_j . Conveniently, an alternative specification of the Palm intensity is

$$\lambda_p(\mathbf{s}_i|\mathbf{s}_j) = \lambda(\mathbf{s}_i)g(\mathbf{s}_i, \mathbf{s}_j), \quad (5)$$

which is the product of the first-order intensity, $\lambda(\mathbf{s}_i)$, and the pair correlation function, $g(\mathbf{s}_i, \mathbf{s}_j)$. An introduction to the Palm distribution for statisticians can be found in Coeurjolly et al. (2017), which includes intuition as well as the measure-theoretic foundations for analyzing its properties.

Likelihood-based inference is an attractive and principled option for statistical analysis. However, many likelihood functions for point processes are intractable due to the presence of normalizing constants that require integration (sometimes stochastic) over a continuous

domain. For an example, consider the inhomogeneous Poisson process with driving intensity $\lambda(\mathbf{s})$. Its log-likelihood is written as

$$\ell(\boldsymbol{\theta}; \mathcal{S}) = \sum_{i=1}^n \log \lambda(\mathbf{s}_i) - \int_D \lambda(\mathbf{u}) d\mathbf{u}. \quad (6)$$

With the exception of a few special cases, the integral for $\lambda(\mathbf{s})$ cannot be found in closed form. In the case of a Cox process, likelihood based inference is complicated further since $\lambda(\mathbf{s})$ is driven by an additional stochastic process. As such, evaluating the likelihood requires integrating over an infinite-dimensional random variable.

Due to this likelihood intractability in many spatial point processes, a common approach is to maximize a simpler objective function that has the advantage of being computationally tractable. For spatial point processes, the Palm likelihood (Ogata & Katsura 1991, Tanaka et al. 2008) is considered a type of pseudolikelihood where its construction arises from the Palm intensity. For example, for the inhomogeneous Poisson process, the log Palm likelihood is written

$$\ell_p(\boldsymbol{\theta}; \mathcal{S}) = \sum_{i \neq j} w_{ij} \log \lambda_p(\mathbf{s}_i | \mathbf{s}_j; \boldsymbol{\theta}) - \int_D w_{uj} \lambda_p(\mathbf{u} | \mathbf{s}_j; \boldsymbol{\theta}) d\mathbf{u} \quad (7)$$

where w_{ij} is a nonnegative weight function, as is commonly seen in composite likelihoods (Varin et al. 2011). In particular, letting $w_{ij} = I\{\|s_i - s_j\| < R\}$ for some distance R , the score of (7) is an asymptotically unbiased estimating equation (Prokešová & Jensen 2013, Baddeley 2017).

Tanaka et al. (2008) first constructed the Palm likelihood for parameter estimation and model selection in Neyman-Scott models. The Palm likelihood is a useful pseudolikelihood approach as it includes both first and second-order intensities. Additionally, this specification is suitable for many different processes which have simple, closed-form expressions and can be used for parameter estimation. Further, asymptotic properties for the maximum Palm likelihood estimator are established in Prokešová & Jensen (2013) under the increasing-

domain framework. Consider an increasing sequence of domains \mathcal{D}_n where all \mathcal{D}_n are convex sets and $\mathcal{D}_n \subseteq \mathcal{D}_{n+1}$ for all $n \in \mathbb{N}$. Denote \mathcal{S}_n as the observed point pattern on \mathcal{D}_n . Letting

$$\hat{\boldsymbol{\theta}}_n = \arg \min_{\boldsymbol{\theta}} \ell_p(\boldsymbol{\theta}; \mathcal{S}_n), \quad (8)$$

$\hat{\boldsymbol{\theta}}_n$ is shown to be asymptotically normal with variance $G^{-1}(\boldsymbol{\theta}_0) = H^{-1}(\boldsymbol{\theta}_0)J(\boldsymbol{\theta}_0)H^{-1}(\boldsymbol{\theta}_0)$. The matrix $G^{-1}(\boldsymbol{\theta}_0)$ is known as the Godambe information ([Godambe 1991](#)), where $H(\boldsymbol{\theta}_0) = E[\frac{d^2}{d\boldsymbol{\theta}^2} \ell_P(\mathcal{S}; \boldsymbol{\theta}_0)]$ and $J(\boldsymbol{\theta}_0) = \text{Var}(\frac{d}{d\boldsymbol{\theta}} \ell_P(\mathcal{S}; \boldsymbol{\theta}_0))$.

While the Palm likelihood can be optimized directly for parameter estimation, when the mean and covariance parameters are separable it is often done in a two-step procedure in practice ([Waagepetersen & Guan 2009](#)). For example, let the parameter vector be defined as $\boldsymbol{\theta} = \{\boldsymbol{\beta}, \boldsymbol{\phi}\}$ where $\boldsymbol{\beta}$ is the vector of mean parameters and $\boldsymbol{\phi}$ is the vector of covariance parameters. The two-step procedure, similar to a profile likelihood approach, starts with estimating $\boldsymbol{\beta}$ by solving the score function

$$\sum_{i=1}^n \frac{d\lambda(\mathbf{s}_i)}{d\boldsymbol{\beta}} \frac{1}{\lambda(\mathbf{s}_i)} - \int_{\mathcal{D}} \frac{d\lambda(\mathbf{u})}{d\boldsymbol{\beta}} d\mathbf{u} = 0. \quad (9)$$

Then, the estimated $\hat{\boldsymbol{\beta}}$ is plugged into (7), which is then solved for $\boldsymbol{\phi}$. This procedure greatly simplifies the optimization process. In the constant mean case of the log-Gaussian Cox process, β_0 (the intercept term in $\boldsymbol{\beta}$) is biased for small values of R when directly optimizing the Palm likelihood ([Dvořák & Prokešová 2012](#)). This shortcoming is overcome with the two-step procedure as the intensity is being estimated directly as if in a homogeneous Poisson process. An important drawback of the two-step procedure is that uncertainty associated with underlying second-order properties is not taken directly into account when estimating standard errors of $\boldsymbol{\beta}$. This two-step procedure is employed in the popular `spatstat` package ([Baddeley & Turner 2005](#)) in CRAN ([R Core Team 2024](#)).

2.2 Examples of Palm intensities

The Palm intensity can be defined in closed form for a suite of different point processes exhibiting the spectrum of clustering to inhibition behaviors. This includes, for example, the log-Gaussian Cox process, the Neyman-Scott process, and the determinantal point process. Simulated realizations from these three point processes are shown in Figure 1. Each of these point patterns exhibit different first and second order structure and yet can be defined by a closed form Palm intensity function. Below we define each of these point processes and specify their Palm intensities.

2.2.1 Log-Gaussian Cox Process

A log-Gaussian Cox process (LGCP) is an inhomogeneous Poisson process with intensity driven by a Gaussian process (GP). Let $W(\mathbf{s})$ denote a mean 0 spatial GP with covariance function parameterized by ϕ . For the moment, define the intensity function at location \mathbf{s} as $\lambda(\mathbf{s}) = \exp\{\beta_0 + W(\mathbf{s})\}$ where β_0 captures the average intensity for all \mathbf{s} . Then, the parameter of interest is the vector $\boldsymbol{\theta} = \{\beta_0, \phi\}$. The Palm intensity for the LGCP can be written

$$\lambda_p(\mathbf{s}_i|\mathbf{s}_j; \boldsymbol{\theta}) = \exp\{\beta_0 + \sigma^2/2 + \sigma^2 \exp\{c(\mathbf{s}_i, \mathbf{s}_j; \phi)\}\} \quad (10)$$

where $c(\mathbf{s}_i, \mathbf{s}_j; \phi) = \text{corr}(W(\mathbf{s}_i), W(\mathbf{s}_j))$, the spatial correlation of the GP between locations \mathbf{s}_i and \mathbf{s}_j . This formulation can be extended to account for covariates by replacing the mean term β_0 with a regression such as $\mathbf{x}(\mathbf{s}_i)' \boldsymbol{\beta}$, where $\mathbf{x}(\mathbf{s}_i)$ is a vector of spatial covariates at location \mathbf{s}_i . Under this specification, the parameter vector becomes $\boldsymbol{\theta} = \{\boldsymbol{\beta}, \phi\}$.

2.2.2 Neyman-Scott Process

The class of Neyman-Scott processes exhibit clustering via parent and offspring points, while assuming stationarity and isotropy. Let $\boldsymbol{\theta} = \{\mu, \nu, \phi\}$. To generate a realization from a Neyman-Scott process, first parent points are generated by a homogeneous Poisson

process with intensity μ . Then, for each generated parent point, the number and location of offspring points are generated. Specifically, the number of offspring points is randomly generated with mean ν and the distances are identically and independently distributed according to a specified density $f_\phi(\mathbf{r})$ where ϕ denotes the parameters indexing the density function and \mathbf{r} is the location vector of the offspring relative to the parent. The collection of offspring points define the realization of the Neyman-Scott process.

Due to stationarity and isotropy, the Palm intensity function is only dependent upon the distance between points, u , giving $\lambda_p(\mathbf{s}_i|\mathbf{s}_j; \boldsymbol{\theta}) = \lambda_p(\|\mathbf{s}_i - \mathbf{s}_j\|) = \lambda_p(u)$. The Palm intensity for a Neyman-Scott process is defined through a relation with the K-function

$$\lambda_p(u) = \lambda g(u) = \frac{\lambda}{2\pi u} \frac{d}{du} K(u) \quad (11)$$

$$\lambda K(u) = \nu \{ \mu \pi u^2 + F_\phi(u) \} \quad (12)$$

where $K(u)$ is Ripley's K-function, $F_\phi(u)$ is the distribution function of the distance between two points within the same cluster, and $\lambda = \mu\nu$ is the overall intensity.

A special case of the Neyman-Scott process is the Thomas process, where $\phi = \sigma^2$ and $f_\phi(\mathbf{r})$ is a bivariate normal density with mean zero and covariance $\sigma^2 \mathbf{I}_2$. For the Thomas process, the Palm intensity can be written

$$\lambda_p(\mathbf{s}_i|\mathbf{s}_j; \boldsymbol{\theta}) = \mu\nu + \frac{\nu}{4\pi\sigma^2} \exp\{-\|\mathbf{s}_i - \mathbf{s}_j\|^2/4\sigma^2\} \quad (13)$$

2.2.3 Determinantal Point Process

Determinantal point processes (DPP) (Lavancier et al. 2015) are inhibition processes that have traditionally found applications in statistical physics and random-matrix theory. Recently, they have seen more use in spatial statistics, where the spatial locations of events reduce the probability of nearby events. Like cluster processes, inhibition processes are described through their second-order structure. Let $C(\mathbf{s}_i, \mathbf{s}_j; \boldsymbol{\theta})$ be a semi-positive definite

kernel defined on $\mathbb{R}^2 \times \mathbb{R}^2$, typically assumed to be a covariance function between locations \mathbf{s}_i and \mathbf{s}_j , and parameterized by $\boldsymbol{\theta}$. Then the n^{th} product density is given by

$$\lambda_n(\mathbf{s}_1, \dots, \mathbf{s}_n) = \det[\Sigma(\boldsymbol{\theta})]. \quad (14)$$

where $\Sigma(\boldsymbol{\theta})$ is the $n \times n$ covariance matrix constructed such that its i, j th element is $C(\mathbf{s}_i, \mathbf{s}_j; \boldsymbol{\theta})$. It follows from this construction that $\lambda(\mathbf{s}) = C(\mathbf{s}, \mathbf{s}; \boldsymbol{\theta})$ and $\lambda_2(\mathbf{s}_i, \mathbf{s}_j) = C(\mathbf{s}_i, \mathbf{s}_i; \boldsymbol{\theta})C(\mathbf{s}_j, \mathbf{s}_j; \boldsymbol{\theta}) - C(\mathbf{s}_i, \mathbf{s}_j; \boldsymbol{\theta})C(\mathbf{s}_j, \mathbf{s}_i; \boldsymbol{\theta})$. Then, the Palm intensity for the DPP can be written

$$\lambda_p(\mathbf{s}_i | \mathbf{s}_j; \boldsymbol{\theta}) = C(\mathbf{s}_i, \mathbf{s}_i; \boldsymbol{\theta}) - \frac{C(\mathbf{s}_i, \mathbf{s}_j; \boldsymbol{\theta})C(\mathbf{s}_j, \mathbf{s}_i; \boldsymbol{\theta})}{C(\mathbf{s}_j, \mathbf{s}_j; \boldsymbol{\theta})}. \quad (15)$$

The tractability of the moments of a DPP is desirable compared to Markov point processes, which have more complex moments requiring approximation. The drawback of these models is that they are slightly less flexible than Gibbs processes (Lavancier et al. 2015), namely in that they cannot replicate the strong regularity of hard-core processes.

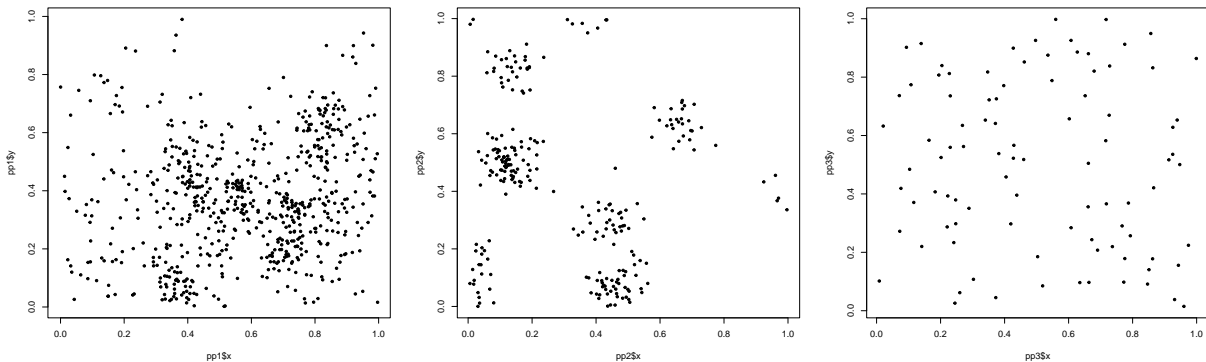


Figure 1: Realizations of (left) LGCP (middle) Thomas process and (right) Determinantal point process with exponential kernel

The simplicity of the Palm intensity expressions for these processes exhibiting radically different behaviors (Figure 1) is attractive for pseudolikelihood-based inference using (7). Palm intensities can also be obtained for Poisson processes, general Cox processes (such

as shot-noise Cox processes (Møller 2003)), and Gibbs processes (Coeurjolly et al. 2017). For Poisson processes, the Palm intensity simplifies to $\lambda_p(\mathbf{s}_i|\mathbf{s}_j) = \lambda(\mathbf{s}_i)$, rendering this procedure unnecessary. Cox processes inherit their moment properties from their latent stochastic processes, meaning the Palm intensity can be computed as long as their first two moments can be obtained. Unfortunately, the Palm intensity for Gibbs processes is not available in closed form (Coeurjolly et al. 2017), necessitating the use of an approximation. Thus, the pseudolikelihood approach for Gibbs processes developed by Baddeley & Turner (2000) remains the most popular inferential technique.

3 Bayesian Inference

3.1 Bayesian Composite Likelihoods

Traditional Bayesian inference relies on deriving (or sampling from) the posterior distribution. Let $\pi(\boldsymbol{\theta})$ define the prior distribution for the model parameters $\boldsymbol{\theta}$. In our setting, the posterior distribution can be written

$$\pi(\boldsymbol{\theta}|\mathcal{S}) \propto L(\boldsymbol{\theta}; \mathcal{S})\pi(\boldsymbol{\theta}). \quad (16)$$

As mentioned above, the likelihood function $L(\boldsymbol{\theta}; \mathcal{S})$ is intractable in the case of many point processes, including the three discussed in Section 2. There is a rich literature on approaches for sampling from posteriors with intractable likelihoods, such as Variational Bayes (Tran et al. 2017) and Approximate Bayesian Computation (ABC) (Sunnåker et al. 2013). Here, we focus on the composite likelihood (Pauli et al. 2011) and more broadly, generalized Bayesian inference (Bissiri et al. 2016). Note that the Palm likelihood is a special case of composite likelihood. We replace the full likelihood $L(\boldsymbol{\theta}; \mathcal{S})$ with the Palm likelihood $L_P(\boldsymbol{\theta}; \mathcal{S})$ to derive the Palm posterior

$$\pi_P(\boldsymbol{\theta}|\mathcal{S}) \propto L_P(\boldsymbol{\theta}; \mathcal{S})\pi(\boldsymbol{\theta}). \quad (17)$$

Chernozhukov & Hong (2003) derived asymptotic properties for this posterior distribution assuming some regularity conditions. Let $\pi_{P,n}(\boldsymbol{\theta}|\mathcal{S}_n)$ be the posterior obtained considering observations on the window \mathcal{D}_n , an increasing sequence of domains (described in Section 2.1). As $n \rightarrow \infty$, the posterior mean accumulates mass around $\hat{\boldsymbol{\theta}}_n$, the maximizer of the objective function (Chernozhukov & Hong 2003). Further, they show that

$$\|\pi_{P,n}(\boldsymbol{\theta}|\mathcal{S}_n) - \pi_{P,\infty}(\boldsymbol{\theta}|\mathcal{S}_\infty)\|_{TV} \xrightarrow{P} 0 \quad (18)$$

as $n \rightarrow \infty$ where $\|\cdot\|_{TV}$ is the total variation norm and $\pi_{P,\infty}(\boldsymbol{\theta}|\mathcal{S})$ is a normal density with variance $H^{-1}(\boldsymbol{\theta}_0)$. Recall that $\hat{\boldsymbol{\theta}}_n$ is asymptotically Normal with variance $G^{-1}(\boldsymbol{\theta}_0) = H^{-1}(\boldsymbol{\theta}_0)J(\boldsymbol{\theta}_0)H^{-1}(\boldsymbol{\theta}_0)$. This implies that the asymptotic variance of the Palm posterior and the asymptotic variance of the Palm likelihood estimator are not equivalent. As such, in order to obtain appropriate posterior inference, defined by nominal coverage of the resulting credible intervals, a posterior adjustment is required (Monahan & Boos 1992). In the next section we propose two different posterior adjustments for Bayesian inference for spatial point patterns using the Palm likelihood.

3.2 Posterior Calibration

Bayesian inference using the Palm likelihood can be shown to result in under-coverage of the posterior distributions of the model parameters. For the parameters of the LGCP, we show the posterior distributions using the full likelihood and Palm likelihood in Figure 2. Heuristically, the invalid frequentist coverage in the generalized Bayesian framework is the result of the information in the likelihood relative to the prior being misrepresented. Under a correctly specified model and likelihood (henceforth full likelihood), the likelihood principle gives that all of the information in the data of size n is represented in the likelihood. In the case of the Palm likelihood, $\binom{n}{2}$ pairs of points are considered independently, thus dramatically inflating the relative strength of the likelihood.

We propose two adjustments to achieve asymptotically valid credible intervals, wherein the $(1 - \alpha)$ credible intervals achieve a Type I error rate of α . The first approach involves raising the Palm likelihood to a fractional power based on theoretical asymptotic behavior in order to down-weight the amount of information present. The second approach offers a direct calibration of the posterior using simulation-based coverage checks.

3.2.1 Adjustment 1 - learning rate adjustment of the likelihood

The first approach aims to modify the likelihood by raising it to a power, or "learning rate," in order to appropriately calibrate the posterior samples. The resulting posterior is written

$$\pi_P(\boldsymbol{\theta}|\mathcal{S}) \propto L_P(\mathcal{S}; \boldsymbol{\theta})^\eta \pi(\boldsymbol{\theta}). \quad (19)$$

This approach naturally appears in a generalized Bayesian framework (Bissiri et al. 2016). We present relevant asymptotic results for the Palm likelihood to justify a particular selection of the "learning rate," denoted η . Then, we propose a procedure for estimating η that is computationally efficient.

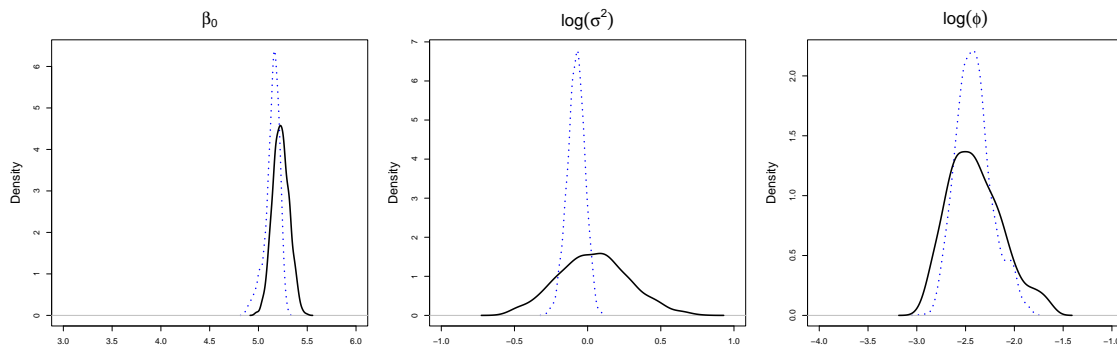


Figure 2: Example of uncalibrated posterior for three parameters of the LGCP. Black line is the posterior under the full likelihood, dashed blue line is the unadjusted posterior derived using the Palm likelihood.

The role of η is to appropriately weight the likelihood relative to the prior, in terms of the amount of information that each provides. As shown in Figure 2, the unadjusted Palm

posterior is too narrow compared to the posterior under the full likelihood for each of the three parameters. An appropriate adjustment aims to *down-weight* the Palm likelihood using $\eta \in (0, 1)$. A survey of approaches to select the learning rate in the more general setting is presented in [Wu & Martin \(2023\)](#) while [Pauli et al. \(2011\)](#) provide an overview specific to composite likelihoods. We adopt the so-called "first-order moment matching" approach ([Geys et al. 1999](#)). This approach was termed the "magnitude adjustment" in [Ribatet et al. \(2012\)](#), who use the composite likelihood in the context of max-stable processes for extreme value analysis. Based on the asymptotic properties of the Palm likelihood ([Prokešová & Jensen 2013](#)), the log-likelihood ratio statistic asymptotically converges to a weighted sum of chi-squared random variables

$$-2\{\ell_P(\mathcal{S}|\boldsymbol{\theta}_0) - \ell_P(\mathcal{S}|\hat{\boldsymbol{\theta}})\} \rightarrow \sum_{i=1}^q \lambda_i \chi_1^2 \quad (20)$$

where λ_i are the eigenvalues of $H(\boldsymbol{\theta}_0)^{-1}J(\boldsymbol{\theta}_0)$. Thus, if we let $\eta = q/\text{tr}(H(\boldsymbol{\theta}_0)^{-1}J(\boldsymbol{\theta}_0))$, then

$$E[-2\{\eta\ell_P(\mathcal{S}|\boldsymbol{\theta}_0) - \eta\ell_P(\mathcal{S}|\hat{\boldsymbol{\theta}})\}] \rightarrow \eta \sum_{i=1}^q \lambda_i = q. \quad (21)$$

Note that the full log-likelihood ratio statistic converges in distribution to a chi-squared distribution with q degrees of freedom. Thus, multiplying by η here results in the first moment of the Palm log-likelihood ratio converging to the same value as the full log-likelihood ratio, theoretically giving us adequate coverage.

Implementing this adjustment requires that we estimate $H(\boldsymbol{\theta}_0)^{-1}J(\boldsymbol{\theta}_0)$. Estimates are difficult to directly obtain because the theoretical expressions contain third and fourth moments of the process. Conveniently, since $H(\boldsymbol{\theta}_0)^{-1}$ is the asymptotic variance of the unadjusted posterior, we can obtain an estimate $\hat{H}(\boldsymbol{\theta}_0)^{-1}$ by fitting the unadjusted model with $\eta = 1$. In the Bayesian framework, we estimate $\hat{H}(\boldsymbol{\theta}_0)^{-1}$ taking the empirical covariance of the resulting posterior samples of $\boldsymbol{\theta}$. Then, an estimate $\hat{J}(\boldsymbol{\theta}_0)$ is obtained via parametric bootstrap using the posterior means initially obtained as the generating parameters. Specif-

ically, a prespecified number B of bootstrapped point patterns $\{\mathcal{S}_1, \dots, \mathcal{S}_B\}$ are generated and the score $\frac{d}{d\boldsymbol{\theta}}\ell_p(\boldsymbol{\theta}; \mathcal{S})$ is calculated for each. The resulting estimator is computed as

$$\hat{J}(\boldsymbol{\theta}_0) = \widehat{Var}\left(\frac{d}{d\boldsymbol{\theta}}\ell_p(\hat{\boldsymbol{\theta}}; \mathcal{S}_i)\right) \quad (22)$$

where $\hat{\boldsymbol{\theta}}$ is the posterior mean with which the bootstrapped point patterns are generated.

3.2.2 Adjustment 2 - matrix adjustment of the posterior samples

The second adjustment we develop calibrates the posterior distribution by scaling each of the posterior samples by a matrix $\boldsymbol{\eta}$. This approach extends the work of [Shaby \(2014\)](#) who proposes scaling (after centering) the posterior draws of $\boldsymbol{\theta}|\mathcal{S}$ obtained via MCMC to achieve desired frequentist coverage. For the j^{th} posterior sample and a scaling matrix $\boldsymbol{\eta}$, we produce a calibrated sample via

$$\tilde{\boldsymbol{\theta}}^{(j)} = \hat{\boldsymbol{\theta}} + \boldsymbol{\eta}(\boldsymbol{\theta}^{(j)} - \hat{\boldsymbol{\theta}}) \quad (23)$$

where $\hat{\boldsymbol{\theta}}$ is the posterior mean. [Shaby \(2014\)](#) uses an asymptotic approach to justify the selection of $\boldsymbol{\eta}$, which he calls the "open-face sandwich adjustment matrix". [Ribatet et al. \(2012\)](#) proposed a similar approach where a "curvature adjustment" to the posterior samples of the parameter vector $\boldsymbol{\theta}$ is applied within each iteration of MCMC and evaluated via the likelihood. Namely, within the Metropolis-Hastings algorithm, each proposal for $\boldsymbol{\theta}^{(j)}$ is transformed via (23) and then $\tilde{\boldsymbol{\theta}}^{(j)}$ is evaluated in the acceptance-rejection step.

Here, we propose an alternative approach to selecting $\boldsymbol{\eta}$ via simulation – namely, a bootstrap approach. Our approach leverages the work of [Syring & Martin \(2019\)](#), who propose a generalized posterior calibration (GPC) approach as a means to select the scalar η (not a matrix as we are now considering) used as a learning rate. As with the previous adjustment, the goal of GPC is to ensure sufficient coverage of credible intervals. To do so, the algorithm uses a nonparametric bootstrap to create B bootstraps datasets. Then the MCMC sampling

algorithm is run using these new datasets with the estimated $\hat{\theta}$ as the "truth". Coverage rates are calculated and, if coverage is unsatisfactory, a new η value is tried and the process continues iteratively until convergence within some tolerance.

For spatial point processes, we modify the GPC algorithm in several ways. Firstly, nonparametric bootstrapping of a point pattern has been studied little in the literature. Therefore, we opt for a parametric bootstrap under the assumed model using $\hat{\theta}$ as the generating parameter values. Secondly, by using the post-hoc adjustment we are able to make the algorithm embarrassingly parallel. This negates the need in [Syring & Martin \(2019\)](#) to iteratively run MCMC to search for η . Lastly, by considering a matrix $\boldsymbol{\eta}$ instead of a scalar learning rate, we allow for unique scalings for each parameter. This is of particular interest because the learning rate approach inflates the uncertainty of all parameters equally, while the information in the data about each parameter is likely to vary substantially, particularly between main effect parameters and those of the covariance function. This results in more accurate empirical coverage of our adjusted posterior distributions for each model parameter. Note that our proposed approach constructs a diagonal matrix $\boldsymbol{\eta}$ in contrast to the approaches of [Ribatet et al. \(2012\)](#) and [Shaby \(2014\)](#) who can have nonzero off-diagonals. Our matrix adjustment approach selects $\boldsymbol{\eta}$ via the modified GPC algorithm presented in [Algorithm 1](#).

3.3 Empirical Prior

Our last contribution is in the form of an empirical prior that mimics the two-step procedure previously mentioned. Consider a spatial point process where the first-order intensity in [\(2\)](#) is a constant, $\lambda(\mathbf{s}) = \lambda$, and the second-order intensity is a function of parameter $\boldsymbol{\theta}$. The `spatstat` package uses a two-step estimation procedure wherein λ is first estimated and then this plugin estimate is used in the Palm likelihood to estimate $\boldsymbol{\theta}$.

Algorithm 1 Modified GPC Algorithm

Require: Observed point pattern \mathcal{S} , number of MCMC samples M , number of bootstrap samples B , coverage level $1 - \alpha$

1: **Step 1: Initial MCMC**

2: Obtain samples $\{\boldsymbol{\theta}^{(1)}, \dots, \boldsymbol{\theta}^{(M)}\}$ from posterior $\pi_P(\boldsymbol{\theta}|\mathcal{S})$ using MCMC

3: Calculate posterior mean $\hat{\boldsymbol{\theta}}$

4: **Step 2: Parametric Bootstrap (parallelize)**

5: Simulate B independent spatial point processes $\mathcal{S}_1, \dots, \mathcal{S}_B$ using $\hat{\boldsymbol{\theta}}$ as the true parameter values.

6: For $k = 1, \dots, B$, obtain samples $\{\boldsymbol{\theta}_k^{(1)}, \dots, \boldsymbol{\theta}_k^{(M)}\}$ from posterior $\pi_P(\boldsymbol{\theta}|\mathcal{S}_k)$ using MCMC

7: **Step 3: Selecting $\boldsymbol{\eta}$**

8: **for** $i = 1$ to q **do**

9: Denote $(1 - \alpha)$ credible region of θ_i from posterior k as $R_{1-\alpha,k}(\theta_i)$

10: Compute:

$$\hat{p}_i = \frac{1}{B} \sum_{k=1}^B I\{\hat{\theta}_i \in R_{1-\alpha,k}(\theta_i)\}$$

11: **if** $\hat{p}_i \geq (1 - \alpha)$ **then**

12: **return** $\eta_i = 1$

13: **else**

14: Let $\tilde{\theta}_i^{(j)} = \hat{\theta}_i + \eta_i(\theta_i^{(j)} - \hat{\theta}_i)$ and denote the resulting credible regions $R_{1-\alpha,k}(\tilde{\theta}_i)$

15: Numerically find η_i such that:

$$\hat{p}_i = \frac{1}{B} \sum_{k=1}^B I\{\hat{\theta}_i \in R_{1-\alpha,k}(\tilde{\theta}_i)\} \geq 1 - \alpha$$

16: **end if**

17: **end for**

18: **Step 4: Calibrate original chain**

19: For $j = 1, \dots, M$, rescale original chain $\{\boldsymbol{\theta}^{(1)}, \dots, \boldsymbol{\theta}^{(M)}\}$

$$\tilde{\boldsymbol{\theta}}^{(j)} = \hat{\boldsymbol{\theta}} + \boldsymbol{\eta}(\boldsymbol{\theta}^{(j)} - \hat{\boldsymbol{\theta}})$$

where

$$\boldsymbol{\eta} = \text{diag}(\eta_1, \dots, \eta_q)$$

We propose an empirical prior to mimic the two-step estimator. First, we reparameterize the Palm intensity as $\lambda_p(\mathbf{s}_i|\mathbf{s}_j; \boldsymbol{\theta}) = \lambda g(\mathbf{s}_i, \mathbf{s}_j; \boldsymbol{\phi})$. Note that the MLE for λ in the homogeneous Poisson process is $\hat{\lambda} = n/|\mathcal{D}|$ where n is the number of observed points. Thus, we construct an empirical prior for λ such that

$$\lambda \sim N(n/|\mathcal{D}|, \sigma_\lambda^2) \tag{24}$$

Importantly, using composition sampling we can recover the posterior distribution of other parameters that are a function of λ , but not explicitly estimated. As an example, in the LGCP, the posterior of β_0 can be obtained as a function of the posteriors of λ and σ^2 , i.e. $\beta_0 = \log(\lambda) - \sigma^2/2$. We explore this empirical prior approach in Section 4.

4 Simulation Study

We now present two simulation studies to examine the efficacy of our approach. First, we simulate from and fit a log-Gaussian Cox process. In fitting using the Palm likelihood, we consider several different distances R , adjustments 1 and 2, and the empirical prior. We then compare our results to those from a full likelihood Bayesian approach in terms of parameter estimation. The second simulation illustrates the utility of the Palm likelihood approach for fitting the Thomas process, a special case of the Neyman-Scott. The Palm likelihood approach in both simulations is executed via a Metropolis-Hastings random walk MCMC.

4.1 Log-Gaussian Cox Process

We simulate 100 spatial point patterns from an LGCP on the domain $\mathcal{D} = [0, 1]^2$ with $E[N(\mathcal{D})] = \lambda = 300$. We define the latent GP as mean 0 with exponential covariance function parameterized by variance $\sigma^2 = 1$ and range $\phi = 0.1$. Following [Diggle et al. \(2013\)](#),

when fitting the model we reparameterize the variance and scale to $\log(\sigma^2)$ and $\log(\phi)$ such that they each have an unconstrained parameter space. Additionally, to facilitate the implementation of the empirical prior, we reparameterize the mean intensity and estimate λ where $\lambda = \exp\{\beta_0 + \sigma^2/2\}$. Posterior estimates of β_0 can be obtained using composition sampling.

For each of the simulated point patterns, we first fit the full likelihood model (FL) and the (unadjusted) Palm likelihood model (PL). For the PL model, we then explore the impact of different choices of the distance R in the Palm Likelihood weights. We consider values of $R \in \{0.2, 0.3, 0.4, 0.5\}$. Finally, we consider the Palm likelihood model with the empirical prior, PLE_R , under the same possible values of R . We use the empirical prior $\lambda \sim N(n, 10)$. For the remaining parameters we use an uninformative normal prior on $\log(\sigma^2)$ and a $\text{Unif}(-3, -1.6)$ prior on $\log(\phi)$.

The posterior distributions for PL and PLE are sampled using an adaptive Metropolis-Hastings algorithm. For FL, the likelihood is intractable due to the infinite dimensional random variable that must be integrated. Therefore, we use a discrete approximation for numerical integration based on a set of k quadrature points, $\mathbf{d}_1, \dots, \mathbf{d}_k$. We assume the intensity function is piecewise constant for each subregion defined by these points. Let W_i denote the GP evaluated at quadrature point \mathbf{d}_i representing a subregion with area $|\mathbf{d}_i|$. Additionally, let $n_i = |\mathcal{S} \cap \mathbf{d}_i|$. We can approximate the log-likelihood as

$$\ell(\beta_0, W; \mathcal{S}) \propto \sum_{i=1}^k n_i(\beta_0 + W_i) - \sum_{i=1}^k |\mathbf{d}_i| \exp\{\beta_0 + W_i\}. \quad (25)$$

which is computationally tractable. In order to sample from the latent GP, we utilize an elliptical slice sampler (Murray et al. 2010).

For each model and simulation, MCMC is run for 20,000 iterations. The first 2,000 samples are discarded as burn-in and the remaining samples are thinned to every 18th, which results in 1,000 samples available for posterior inference.

The primary appeal of our approach is the computational scalability, which we assess using effective sample size per second. Table 1 shows the effective sample size per second for each model, where $PL_{0.2}$ is shown to perform the best for two of the three parameters. In general, the effective sample size per second decreases as R increases. Note that this is the ESS/second before adjusting the posterior. For $PL_{0.2}$, we found that the learning rate adjustment took 47.11 seconds on average and the GPC adjustment took 40.35 seconds on average, compared to an average 23.52 seconds for the unadjusted Palm posterior. Even with this increase in computation time, we can see that the Palm likelihood approach is orders of magnitude faster than the full likelihood MCMC with elliptical slice sampler.

Model	β_0	σ^2	ϕ
FL	0.13	0.12	0.13
$PL_{0.2}$	12.37	25.76	7.14
$PL_{0.3}$	17.18	17.10	6.17
$PL_{0.4}$	14.18	12.16	6.47
$PL_{0.5}$	11.01	9.45	6.04

Table 1: Effective sample size per second

To evaluate the estimation performance of each model we compute the bias and RMSE of the posterior mean with respect to the parameters of interest. These values are reported in Table 2 for each model being compared. As expected, FL performs the best with small bias and the lowest RMSE for each parameter. However, $PL_{0.2}$ performs equally well in terms of bias with only marginally higher RMSE than FL. This indicates a significant improvement using the empirical prior in the case of the LGCP for parameter estimation. Under PL, we detect a slight increase in bias as R increases. This result contrasts the findings of [Dvořák & Prokešová \(2012\)](#) who, within a frequentist context of optimizing the

Palm likelihood, find bias to decrease as R increases. Finally, the increase in RMSE under the PL models indicates more uncertainty in parameter estimation when compared to the FL model.

Model	Bias			RMSE		
	β_0	σ^2	ϕ	β_0	σ^2	ϕ
FL	-0.01	0.07	0.01	0.10	0.27	0.02
PL _{0.2}	-0.12	0.05	0.00	0.32	0.38	0.04
PL _{0.3}	-0.14	0.07	0.01	0.32	0.40	0.04
PL _{0.4}	-0.15	0.08	0.01	0.31	0.41	0.05
PL _{0.5}	-0.16	0.09	0.01	0.31	0.42	0.05
PLE _{0.2}	-0.01	0.00	-0.01	0.15	0.33	0.04
PLE _{0.3}	-0.05	0.04	-0.01	0.18	0.36	0.04
PLE _{0.4}	-0.08	0.06	-0.01	0.21	0.38	0.04
PLE _{0.5}	-0.11	0.08	0.00	0.22	0.39	0.04

Table 2: Posterior mean bias and RMSE for the LGCP across models.

Next, we apply the learning rate adjustment and matrix adjustment to calibrate the widths of our posterior distributions for each parameter to ensure proper coverage. Figure 3 illustrates how adjustment 2 (GPC) widens the unadjusted posterior for a single simulation run. In general, the adjusted posteriors tend to be more diffuse than those from FL model. This is to be expected as the Palm likelihood is a pseudolikelihood that loses some information when compared to the full likelihood, as shown previously with the inflated RMSEs.

Table 3 shows the empirical coverages of FL along with the unadjusted and adjusted versions of PL and PLE. As we can see, adjustment 1 (learning rate with asymptotic justification) significantly over-covers the nominal coverage level, whereas adjustment 2 (GPC) seems to

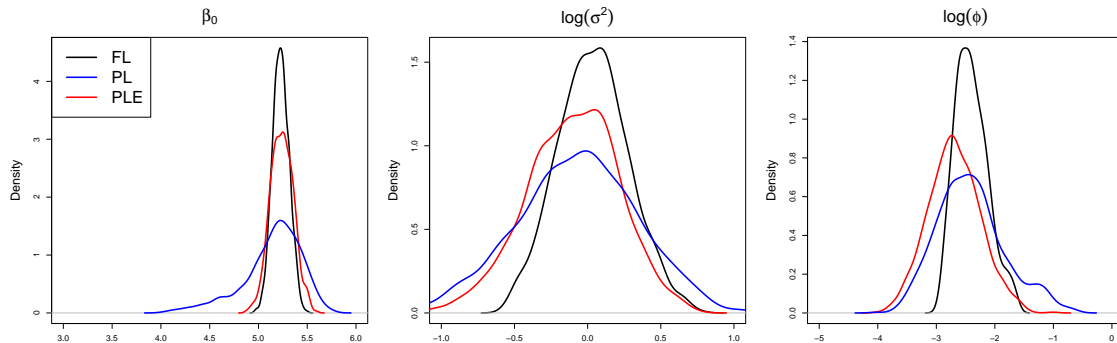


Figure 3: Example of posterior adjustment for three parameters of the LGCP. Black line is the posterior under the full likelihood, blue line is the GPC adjusted posteriors for non-empirical, and red line the GPC adjusted posteriors for the empirical prior.

perform as well as FL. The dramatic undercovering of the unadjusted posteriors further illustrates why these adjustments are necessary.

Though adjustment 1 has sound theoretical justification, in practice it is difficult to estimate the covariance matrix of the maximum Palm likelihood estimator and that difficulty translates to too small of an η , giving larger credible intervals, as can be seen in the median credible interval lengths in parentheses.

4.2 Thomas Process

To illustrate the generality of our approach, a second simulation study uses the Thomas process. The Thomas process is a special case of the Neyman-Scott process described in Section 2.2.2, where the offspring points are distributed according to a bivariate Gaussian distribution. The resulting $f_{\theta}(\mathbf{r})$ is given by

$$f_{\theta}(\mathbf{r}) = \frac{1}{2\pi\sigma^2} e^{-\frac{\mathbf{r}'\mathbf{r}}{2\sigma^2}}, \quad (26)$$

which gives the palm intensity

$$\lambda_p(u) = \mu\nu + \frac{\nu}{4\pi^2\sigma^2} e^{-\frac{u^2}{4\sigma^2}} \quad (27)$$

Model	β_0	σ^2	ϕ
FL	0.93 (0.36)	0.91 (0.92)	0.93 (1.00)
PL	0.30 (0.28)	0.34 (0.23)	0.54 (0.54)
PLE	0.31 (0.11)	0.26 (0.20)	0.18 (0.23)
PL ⁽¹⁾	1.00 (1.08)	1.00 (2.65)	1.00 (1.32)
PL ⁽²⁾	0.95 (1.20)	0.90 (1.41)	0.93 (1.95)
PLE ⁽¹⁾	1.00 (0.84)	0.99 (2.55)	0.99 (1.31)
PLE ⁽²⁾	0.88 (0.55)	0.88 (1.23)	0.86 (1.63)

Table 3: 95% empirical credible interval coverage of LGCP parameter posteriors with associated median interval lengths in parentheses

We simulate 100 point patterns from a Thomas process with generating parameters $\mu = 10, \nu = 30, \sigma^2 = 0.0025$ using the `spatstat` package. Similar to the LGCP, we reparameterize each parameter to the log scale and again model the λ parameter where we can obtain the posterior distribution for ν via composition sampling with $\lambda = \mu\nu$. Uninformative normal priors are used for all three parameters. We choose $R = 0.2$ because of the balance of computational and statistical performance shown in the LGCP study for this threshold.

Model	Bias			RMSE		
	μ	ν	σ^2	μ	ν	σ^2
PL _{0.2}	0.60	1.46	0.26*	16.34	5.61	1.17*
PLE _{0.2}	4.86	0.08	0.04*	15.57	4.93	1.27*

* Denotes 10^{-3}

Table 4: Posterior mean bias and RMSE for the Thomas process across models.

Table 4 shows the bias and RMSE of the posterior mean parameter estimates across the 100 simulated datasets. Here, the non-empirical version performs better than the empirical version with respect to bias when estimating μ . $\text{PLE}_{0.2}$ on the other hand performs better with respect to bias for ν . RMSE is comparable across models for each parameter, which contrasts what we saw under the LGCP; however, they both perform adequately.

Model	μ	ν	σ^2
PL	0.40	0.40	0.48
PLE	0.21	0.16	0.23
PL ⁽¹⁾	1.00	1.00	1.00
PL ⁽²⁾	0.95	0.93	0.95
PLE ⁽¹⁾	1.00	1.00	1.00
PLE ⁽²⁾	0.90	0.90	0.88

Table 5: 95% empirical credible interval coverage of Thomas process parameters

With regards to adjustment 1, the approach dramatically underweights the likelihood resulting in a virtual return to the prior and overcoverage. Alternatively, the GPC adjustment improves coverage relative to the unadjusted version, reaching the nominal 95% coverage level. Similar to the results of the first simulation, the empirical version under adjustment 2 slightly undercovers the true parameter values. Based on these simulations we recommend the Thomas process be approached with an uninformative prior and utilizing the GPC adjustment.

5 Data Analysis

We apply our approach to the `bei` dataset found in `spatstat`. This dataset consists of 3605 *Beilschmiedia pendula Lauraceae* trees located in the rainforest of Barro Colorado island within a $1000\text{m} \times 500\text{m}$ spatial domain. The locations are shown spatially in Figure 4. This dataset has been analyzed previously in the literature using other approaches (Møller & Waagepetersen 2007, Flagg & Hoegh 2023). Spatial point patterns are often studied in forestry to detect important drivers of the spatial distribution of a particular species across a spatial region (Stoyan & Penttinen 2000, Comas & Mateu 2007). In our analysis we consider two possible explanatory variables, elevation and gradient, which are assumed to be possible drivers of the distribution of this tree species. Elevation and gradient are shown spatially in Figure 4.

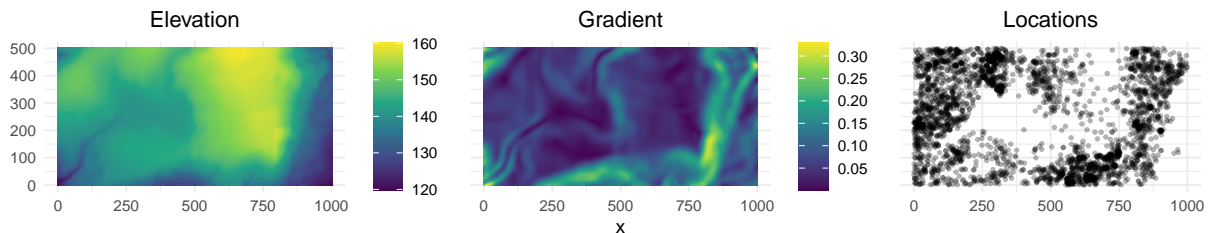


Figure 4: Maps of spatial covariates, elevation and gradient, and the locations of *Beilschmiedia pendula Lauraceae* trees.

We proceed by fitting an LGCP with covariates in the intensity function. Let $\mathcal{S} = \{\mathbf{s}_1, \dots, \mathbf{s}_n\}$ be the locations of trees with $n = 3605$, $W(\mathbf{s}_i)$ be the zero-mean latent Gaussian process at point \mathbf{s}_i , and $\mathbf{x}(\mathbf{s}_i)$ be the vector of covariates (including an intercept term) at location \mathbf{s}_i . We assume \mathcal{S} comes from an LGCP with log-intensity

$$\log \lambda(\mathbf{s}) = \mathbf{x}(\mathbf{s})' \boldsymbol{\beta} + W(\mathbf{s}) \quad (28)$$

$$\mathbf{W} \sim GP(\mathbf{0}, \boldsymbol{\Sigma}) \quad (29)$$

	β_0	β_1	β_2	σ^2	ϕ
MW	N/A	0.06(0.02, 0.10)	8.76(6.03, 11.37)	2.59(2.07, 3.42)	42.5(32.10, 56.45)
FH	-10.9(-14.2, -7.63)	0.03(0.01, 0.05)	4.44(2.42, 6.46)	1.69(1.10, 2.66)	176(137, 229)
PL ₂₀₀	-8.98(-15.55, -1.71)	0.02(-0.02, 0.07)	4.36(-3.58, 11.70)	1.29(0.90, 1.80)	63.84(31.76, 149.22)

Table 6: Posterior means along with 95% credible intervals in parantheses for parameters in LGCP model of *Beilschmiedia pendula Lauraceae*.

where the covariance matrix, Σ , is defined by an exponential covariance function such that $Cov(W(\mathbf{s}_i), W(\mathbf{s}_j)) = \sigma^2 \exp\{\|\mathbf{s}_i - \mathbf{s}_j\|/\phi\}$. The parameters of interest are $\boldsymbol{\beta} = \{\beta_0, \beta_1, \beta_2\}$, σ^2 , and ϕ . For this model, the Palm intensity is written

$$\lambda_p(s_i | s_j; \boldsymbol{\theta}) = \exp\{\mathbf{x}(\mathbf{s}_i)' \boldsymbol{\beta} + \sigma^2/2 + \sigma^2 \exp\{\|\mathbf{s}_i - \mathbf{s}_j\|/\phi\}\} \quad (30)$$

and $w_{ij} = I\{\|\mathbf{s}_i - \mathbf{s}_j\| \leq R\}$.

To complete the Bayesian hierarchical model framework, we assign prior distributions to all model parameters. The regression coefficients β_0 , β_1 , and β_2 are each assigned a independent, uninformative $N(0, 1000)$ priors. Additionally, $\log(\sigma^2) \sim N(0, 10)$, and $\log(\phi) \sim Unif(\log(20), \log(200))$. We set $R = 200$, which is 20% of the long side of the rectangular region. An adaptive Metropolis-Hastings algorithm is used to sample from the resulting posteriors.

We compare our results to [Flagg & Hoegh \(2023\)](#) and [Møller & Waagepetersen \(2007\)](#) who use INLA and a fully Bayesian approach for model inference, respectively. Each of these analyses assume different prior distributions on the parameters, but all are relatively uninformative priors. The only difference in model specification is that [Flagg & Hoegh \(2023\)](#) use a Matérn covariance function with smoothness parameter $\nu = 1$, whereas $\nu = 1/2$ (the exponential covariance function) here and in [Møller & Waagepetersen \(2007\)](#).

The results shown in Table 6 are labeled as MW for [Møller & Waagepetersen \(2007\)](#), FH for [Flagg & Hoegh \(2023\)](#), and PL₂₀₀ for our approach. Posterior means and 95%

credible intervals are reported. Note that the intercept β_0 was not reported in Møller & Waagepetersen (2007). Overall, we obtain similar results to the other analyses conducted with different methodologies. The most notable difference is that our approach has greater uncertainty, particularly for the β_1 and β_2 posteriors. This is to be expected based on our previous discussions. Although these coefficients may not be deemed "significant" at the 95% level, these credible regions still provide evidence of a positive effect from elevation and gradient on tree intensity. Another notable difference is that the FH estimate of ϕ is larger than the other approaches, which we attribute to the difference in smoothness parameters used.

6 Discussion

In this paper, we have developed an approach for spatial point pattern analysis using the Palm likelihood in a generalized Bayesian framework. Motivated by the intractability of the full likelihood for many different point processes, we explored the efficacy of Palm likelihoods for Bayesian parametric inference. It was shown through simulation studies that significant computational gains in MCMC algorithms are achieved with this method. However, a drawback is that the immediate posterior uncertainty when using the Palm likelihood does not provide adequate frequentist coverage. In order to remedy this shortcoming, we propose two different adjustments to calibrate the posterior. One modifies the "weight" of the likelihood using asymptotically justified estimates, while the other directly modifies the posterior samples using the modified GPC algorithm. Through simulation, we find the second adjustment to perform best, whereas the first is generally too conservative. Additionally, we notice some inherent bias in estimating the mean intensity, which we remedy by proposing an empirical prior to mimic traditional two-step estimation.

The primary limitation of our work is that the inherent uncertainty (after calibration) when

using the Palm likelihood is greater than under the fully Bayesian approach. This inefficiency can be attributed to the general loss of information that comes with using pseudolikelihoods in any context. However, given that our method is fast and easy to implement across a number of point process models, it is particularly useful for model selection and comparison in preliminary analysis.

This paper is a first step into applying the generalized Bayesian framework to point pattern analysis. Future work includes comparing the performance of composite likelihoods (Guan 2006) to the Palm likelihood in a Bayesian context, or even more general optimal estimating equations (Møller & Waagepetersen 2017). Similarly, under the paradigm of Bissiri et al. (2016), one could update prior beliefs under any loss function, such as the minimum contrast estimator (1). Although the determinantal point process characterizes inhibition, Markov point processes are considered to be more flexible and are more commonly applied in the literature. Future work looks to extend our method using the pseudolikelihood for Gibbs processes (Baddeley & Turner 2000). Finally, different approaches for calibrating general posteriors have been developed (Wu & Martin 2023) and could be tested in this context.

7 Disclosure statement

The authors have no conflicts of interest to declare.

8 Data Availability Statement

Data is available in the `spatstat` R package (`bei`).

SUPPLEMENTARY MATERIAL

Code: The code to produce the simulation study, real data analysis, and all resulting

figures/tables. (BayesianPalm_code.zip, .zip)

References

- Baddeley, A. (2017), ‘Local composite likelihood for spatial point processes’, *Spatial Statistics* **22**, 261–295.
- Baddeley, A., Rubak, E. & Turner, R. (2016), *Spatial point patterns: methodology and applications with R*, Vol. 1, CRC press Boca Raton.
- Baddeley, A. & Turner, R. (2000), ‘Practical maximum pseudolikelihood for spatial point patterns: (with discussion)’, *Australian & New Zealand Journal of Statistics* **42**(3), 283–322.
- Baddeley, A. & Turner, R. (2005), ‘Spatstat: an R package for analyzing spatial point patterns’, *Journal of Statistical Software* **12**, 1–42.
- Ben-Said, M. (2021), ‘Spatial point-pattern analysis as a powerful tool in identifying pattern-process relationships in plant ecology: an updated review’, *Ecological Processes* **10**, 1–23.
- Besag, J. (1974), ‘Spatial interaction and the statistical analysis of lattice systems’, *Journal of the Royal Statistical Society: Series B (Methodological)* **36**(2), 192–225.
- Betancourt, M. (2017), ‘A conceptual introduction to Hamiltonian Monte Carlo’, *arXiv preprint arXiv:1701.02434* .
- Bevilacqua, M., Gaetan, C., Mateu, J. & Porcu, E. (2012), ‘Estimating space and space-time covariance functions for large data sets: a weighted composite likelihood approach’, *Journal of the American Statistical Association* **107**(497), 268–280.
- Bissiri, P. G., Holmes, C. C. & Walker, S. G. (2016), ‘A general framework for updating belief

- distributions', *Journal of the Royal Statistical Society Series B: Statistical Methodology* **78**(5), 1103–1130.
- Burguet, J. & Andrey, P. (2014), 'Statistical comparison of spatial point patterns in biological imaging', *PLoS One* **9**(2), e87759.
- Chernozhukov, V. & Hong, H. (2003), 'An MCMC approach to classical estimation', *Journal of Econometrics* **115**(2), 293–346.
- Coeurjolly, J.-F., Møller, J. & Waagepetersen, R. (2017), 'A tutorial on palm distributions for spatial point processes', *International Statistical Review* **85**(3), 404–420.
- Comas, C. & Mateu, J. (2007), 'Modelling forest dynamics: a perspective from point process methods', *Biometrical Journal: Journal of Mathematical Methods in Biosciences* **49**(2), 176–196.
- Curriero, F. C. & Lele, S. (1999), 'A composite likelihood approach to semivariogram estimation', *Journal of Agricultural, Biological, and Environmental Statistics* pp. 9–28.
- D'Angelo, N., Adelfio, G. & Mateu, J. (2023), 'Locally weighted minimum contrast estimation for spatio-temporal log-Gaussian Cox processes', *Computational Statistics & Data Analysis* **180**, 107679.
- Diggle, P. J. (2013), *Statistical analysis of spatial and spatio-temporal point patterns*, CRC press.
- Diggle, P. J., Moraga, P., Rowlingson, B. & Taylor, B. M. (2013), 'Spatial and spatio-temporal log-Gaussian Cox processes: extending the geostatistical paradigm'.
- Dvořák, J. & Prokešová, M. (2012), 'Moment estimation methods for stationary spatial Cox processes-a comparison', *Kybernetika* **48**(5), 1007–1026.

- Flagg, K. & Hoegh, A. (2023), ‘The integrated nested Laplace approximation applied to spatial log-Gaussian Cox process models’, *Journal of Applied Statistics* **50**(5), 1128–1151.
- Gelfand, A. E. & Schliep, E. M. (2018), Bayesian inference and computing for spatial point patterns, in ‘NSF-CBMS regional conference series in probability and statistics’, Vol. 10, JSTOR, pp. i–125.
- Geys, H., Molenberghs, G. & Ryan, L. M. (1999), ‘Pseudolikelihood modeling of multivariate outcomes in developmental toxicology’, *Journal of the American Statistical Association* **94**(447), 734–745.
- Godambe, V. P., ed. (1991), *Estimating Functions*, Oxford University Press.
- Guan, Y. (2006), ‘A composite likelihood approach in fitting spatial point process models’, *Journal of the American Statistical Association* **101**(476), 1502–1512.
- Kleijn, B. J. & Van der Vaart, A. W. (2012), ‘The Bernstein-von-Mises theorem under misspecification’, *Electronic Journal of Statistics* .
- Kopecký, J. & Mrkvička, T. (2016), ‘On the Bayesian estimation for the stationary Neyman-Scott point processes’, *Applications of Mathematics* **61**(4), 503–514.
- Lavancier, F., Møller, J. & Rubak, E. (2015), ‘Determinantal point process models and statistical inference’, *Journal of the Royal Statistical Society Series B: Statistical Methodology* **77**(4), 853–877.
- Lindsay, B. G. (1988), Composite likelihood methods, in ‘Statistical Inference from Stochastic Processes: Proceedings of the AMS-IMS-SIAM Joint Summer Research Conference Held August 9-15, 1987, with Support from the National Science Foundation and the Army Research Office’, Vol. 80, American Mathematical Soc., p. 221.
- Martin, R. & Syring, N. (2022), Direct Gibbs posterior inference on risk minimizers:

- Construction, concentration, and calibration, *in* ‘Handbook of Statistics’, Vol. 47, Elsevier, pp. 1–41.
- Møller, J. (2003), ‘Shot noise Cox processes’, *Advances in Applied Probability* **35**(3), 614–640.
- Møller, J., Syversveen, A. R. & Waagepetersen, R. P. (1998), ‘Log Gaussian Cox Processes’, *Scandinavian Journal of Statistics* **25**(3), 451–482.
- Møller, J. & Waagepetersen, R. (2007), ‘Modern spatial point process modelling and inference (with discussion)’, *Scandinavian Journal of Statistics* **34**, 643–711.
- Møller, J. & Waagepetersen, R. (2017), ‘Some recent developments in statistics for spatial point patterns’, *Annual Review of Statistics and Its Application* **4**(1), 317–342.
- Møller, J. & Waagepetersen, R. P. (2003), *Statistical inference and simulation for spatial point processes*, CRC press.
- Monahan, J. F. & Boos, D. D. (1992), ‘Proper likelihoods for Bayesian analysis’, *Biometrika* **79**(2), 271–278.
- Murray, I., Adams, R. & MacKay, D. (2010), Elliptical slice sampling, *in* ‘Proceedings of the thirteenth international conference on artificial intelligence and statistics’, JMLR Workshop and Conference Proceedings, pp. 541–548.
- Ogata, Y. & Katsura, K. (1991), ‘Maximum likelihood estimates of the fractal dimension for random spatial patterns’, *Biometrika* pp. 463–474.
- Pauli, F., Racugno, W. & Ventura, L. (2011), ‘Bayesian composite marginal likelihoods’, *Statistica Sinica* pp. 149–164.
- Perry, G. L., Miller, B. P. & Enright, N. J. (2006), ‘A comparison of methods for the statistical analysis of spatial point patterns in plant ecology’, *Plant Ecology* **187**, 59–82.

- Prokešová, M. & Jensen, E. B. V. (2013), ‘Asymptotic palm likelihood theory for stationary point processes’, *Annals of the Institute of Statistical Mathematics* **65**(2), 387–412.
- R Core Team (2024), *R: A Language and Environment for Statistical Computing*, R Foundation for Statistical Computing, Vienna, Austria.
- URL:** <https://www.R-project.org/>
- Ribatet, M., Cooley, D. & Davison, A. C. (2012), ‘Bayesian inference from composite likelihoods, with an application to spatial extremes’, *Statistica Sinica* pp. 813–845.
- Rue, H., Riebler, A., Sørbye, S. H., Illian, J. B., Simpson, D. P. & Lindgren, F. K. (2017), ‘Bayesian computing with INLA: a review’, *Annual Review of Statistics and Its Application* **4**(1), 395–421.
- Schliep, E. M., Wikle, C. K. & Daw, R. (2023), ‘Correcting for informative sampling in spatial covariance estimation and kriging predictions’, *Journal of Geographical Systems* **25**(4), 587–613.
- Shaby, B. A. (2014), ‘The open-faced sandwich adjustment for MCMC using estimating functions’, *Journal of Computational and Graphical Statistics* **23**(3), 853–876.
- Shirota, S. & Gelfand, A. E. (2017), ‘Space and circular time log Gaussian Cox processes with application to crime event data’, *The Annals of Applied Statistics* pp. 481–503.
- Stoyan, D. & Penttinen, A. (2000), ‘Recent applications of point process methods in forestry statistics’, *Statistical Science* pp. 61–78.
- Sunnåker, M., Busetto, A. G., Numminen, E., Corander, J., Foll, M. & Dessimoz, C. (2013), ‘Approximate Bayesian computation’, *PLoS Computational Biology* **9**(1), e1002803.
- Syring, N. & Martin, R. (2019), ‘Calibrating general posterior credible regions’, *Biometrika* **106**(2), 479–486.

- Tanaka, U., Ogata, Y. & Stoyan, D. (2008), ‘Parameter estimation and model selection for Neyman-Scott point processes’, *Biometrical Journal: Journal of Mathematical Methods in Biosciences* **50**(1), 43–57.
- Teng, M., Nathoo, F. & Johnson, T. D. (2017), ‘Bayesian computation for log-Gaussian Cox processes: A comparative analysis of methods’, *Journal of Statistical Computation and Simulation* **87**(11), 2227–2252.
- Tran, M.-N., Nott, D. J. & Kohn, R. (2017), ‘Variational Bayes with intractable likelihood’, *Journal of Computational and Graphical Statistics* **26**(4), 873–882.
- Varin, C., Reid, N. & Firth, D. (2011), ‘An overview of composite likelihood methods’, *Statistica Sinica* pp. 5–42.
- Velázquez, E., Martínez, I., Getzin, S., Moloney, K. A. & Wiegand, T. (2016), ‘An evaluation of the state of spatial point pattern analysis in ecology’, *Ecography* **39**(11), 1042–1055.
- Waagepetersen, R. & Guan, Y. (2009), ‘Two-step estimation for inhomogeneous spatial point processes’, *Journal of the Royal Statistical Society Series B: Statistical Methodology* **71**(3), 685–702.
- Waagepetersen, R., Guan, Y., Jalilian, A. & Mateu, J. (2016), ‘Analysis of multispecies point patterns by using multivariate log-gaussian cox processes’, *Journal of the Royal Statistical Society Series C: Applied Statistics* **65**(1), 77–96.
- Weston, D. J., Adams, N. M., Russell, R. A., Stephens, D. A. & Freemont, P. S. (2012), ‘Analysis of spatial point patterns in nuclear biology’, *PLoS One* **7**(5), e36841.
- Wu, P.-S. & Martin, R. (2023), ‘A comparison of learning rate selection methods in generalized bayesian inference’, *Bayesian Analysis* **18**(1), 105–132.